Journal of Loss Prevention in the Process Industries 26 (2013) 32–37

Contents lists available at SciVerse ScienceDirect

Journal of Loss Prevention in the Process Industries

journal homepage: www.elsevier.com/locate/jlp

Investigation of the properties of the accidental release and explosion of liquefied dimethyl ether at a filling station

Toshio Mogi [a,*], Hiroumi Shiina [b], Yuji Wada [b], Ritsu Dobashi [a]

[a] Graduate School of Engineering, The University of Tokyo, 7-3-1, Hongo, Bukyo-ku, Tokyo 113-8656, Japan
[b] Research Institute of Science for Safety and Sustainability (RISS), National Institute of Advanced Industrial Science and Technology (AIST), 16-1, Onogawa, Tsukuba, Ibaraki 305-8569, Japan

ARTICLE INFO

Article history:
Received 6 January 2012
Received in revised form
22 August 2012
Accepted 2 September 2012

Keywords:
Dimethyl ether
DME
Flame propagation
Blast wave
Heat flux
Fireball

ABSTRACT

Dimethyl ether (DME) has been focused as a substitute for diesel fuel, and a number of studies have investigated engines fueled with DME because DME has a low auto-ignition temperature and does not generate particulate matter (PM). Therefore, in the last few years, the construction of DME filling stations for trucks in Japan has been planned. The introduction of DME vehicles requires expansion of DME supply stations, which in turn requires the collection of safety data and the establishment of safety regulations. The present paper describes an experimental investigation of the hypothetical scenario in which liquid DME is accidentally released and an explosion occurs. In the present study, large-scale leakage and ignition of DME were investigated and flame propagation data was obtained. We also measured the overpressure of the blast wave and the heat flux from the fireball. When the ignition position is near the nozzle, the flame propagation velocity is higher. The overpressure from the DME fireball is stronger than that from DME/air mixture deflagration. In summary, these results provide safety data for safety management of DME filling stations.

1. Introduction

Dimethyl ether (DME) has been focused as a substitute for diesel fuel because it has a low auto-ignition temperature and can reduce the emission of NO_x, SO_x, and particulate matter. As such, a number of studies on engines fueled with DME have been conducted (Suha & Lee, 2008; Yamada, Yoshii, & Tezaki, 2005; Ying, Li, Jie, & Longbao, 2009), and diesel engines that run on DME have been developed. Moreover, in recent years, the widespread construction of DME filling stations has been planned in Japan. However, since DME has been primarily used as an aerosol propellant, there is little data available on the use of DME as a fuel. Therefore, the preparation of safety regulations, such as safety distances for DME infrastructure, such as DME supply stations, is very important, and obtaining such safety data is necessitated by the increase in the number of DME filling stations and vehicles fueled with DME. Although a number of studies have been conducted to examine the properties and combustion characteristics of DME (Daly, Simmie, & Wurmel, 2001; Huang et al., 2007; Zhao, Kazakov, & Dryer, 2004), a very small number of studies have conducted experimental investigations on safety. Nifuku et al. (2006) have reported the static electrification characteristics of DME. Mogi and Horiguchi (2009) experimentally investigated the explosion and detonation characteristics of DME.

Dimethyl ether filling facilities should have a safety coupling on the supply hose. This coupling can become separated when a driver accidentally leaves the supply hose attached to the vehicle, preventing the hose from being broken and spilling DME. However, as one of the postulated disaster scenarios, a hose is broken and DME is discharged rapidly because the safety coupling fails. Then, leaking DME is ignited by an ignition source such as an electrostatic spark discharge, and an explosion and fire occur. Dimethyl ether has similar physical properties to liquefied petroleum gas (LPG). For example, DME is easily liquefied by applying a pressure of 0.53 MPa at 293 K. Therefore, if a major liquid DME leak occurs, upon release of liquid DME, a DME vapor cloud will formed. Vapor cloud explosions (VCEs) will then likely occur, as in the cased of LPG release accidents (Bubbico & Marchini, 2008). However, few studies have examined the release and explosion of liquid DME leaking due to a large-scale pipe break, and blows down to atmosphere were reported.

The aim of the present study was to investigate the hazards of DME assuming accidental leakage at a DME filling station. The tests simulated rapid and large-scale leakage as a result of breakage of

* Corresponding author. Tel.: +81 3 5841 1837; fax: +81 3 3815 8359.
E-mail addresses: mogi.toshio@mail.u-tokyo.ac.jp, godspeed@js4.so-net.ne.jp (T. Mogi).

0950-4230/$ – see front matter
http://dx.doi.org/10.1016/j.jlp.2012.09.002

piping connecting, for example, filling facilities, and storage tanks. Field tests were carried out in order to clarify the leakage, dispersion, and explosion behaviors. Flame propagation in the DME jet in the event of ignition was observed. Furthermore, we measured the overpressure of the blast wave and the heat flux from the fireball.

2. Experimental apparatus and procedures

Fig. 1 shows a schematic diagram of the experimental apparatus. Liquid DME was stored in a tube having a capacity of 1.4 L as a storage tank. The operating pressure of the planned DME supply systems is higher than the vapor pressure of DME (0.59 MPa at 298 K). Therefore, the present study, the pressure of DME was raised by nitrogen gas to 2 MPa. Dimethyl ether was ejected horizontally through a 19 mm diameter stainless steel tube at a height of 1 m from the release position.

Ignition was performed with a pilot burner or an electric spark positioned along the discharge axis at a distance of 0.2–8 m from the nozzle and 1 m above the ground surface. A torch burner fueled by LPG was used as a pilot burner. The burner was ignited before the DME was released and was extinguished as soon as the DME jet was ignited. An electric spark was generated by the discharge electrode with a 3.5 mm gap and a neon sign transformer (15 kV, 20 mA).

The stagnant pressure, p_0, in the header was measured by a strain-gage-type pressure transducer (KYOWA, PHL-A-10MP-B), which was connected to a dynamic strain amplifier (KYOWA, CDV-700A). Measurements of pressure, radiant heat, and imaging were conducted at the locations indicated in Fig. 2. The distance between the ignition position and each pressure sensor differed in each experiment because the pressure sensors were fixed. The propagating flame was recorded using a digital video camera (SONY, DSR-PD170A, 30 fps). Furthermore, IR wavelength images were obtained using an IR-sensitive digital video camera (SONY, DCR-TRV107, 30 fps) with a 950 nm lower cutoff filter because the luminance from the DME flame was relatively weak. The blast wave pressures generated by the explosion of the jet at the time of discharge were measured by silicon diaphragm pressure transducers (Kulite, XT-190-5SG). Each pressure sensor was positioned on the DME jet axis. Radiant heat sensors (Captec Enterprise, RF-30, response time 100 ms) were used to evaluate the thermal radiation from the DME flame. Output signals from the pressure sensors and the radiant heat sensors were recorded using a digital oscilloscope (HIOKI, MEMORY HiCORDER 8861).

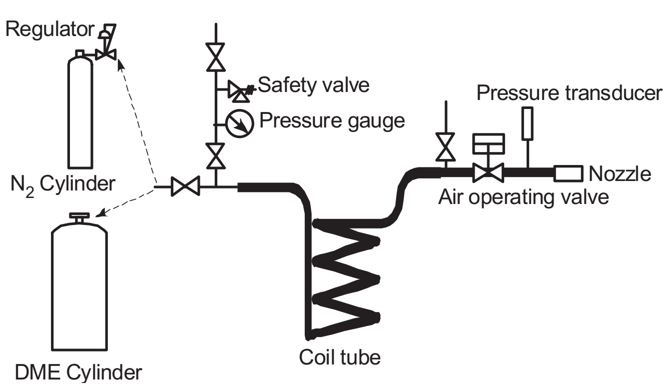

Fig. 1. Experimental apparatus.

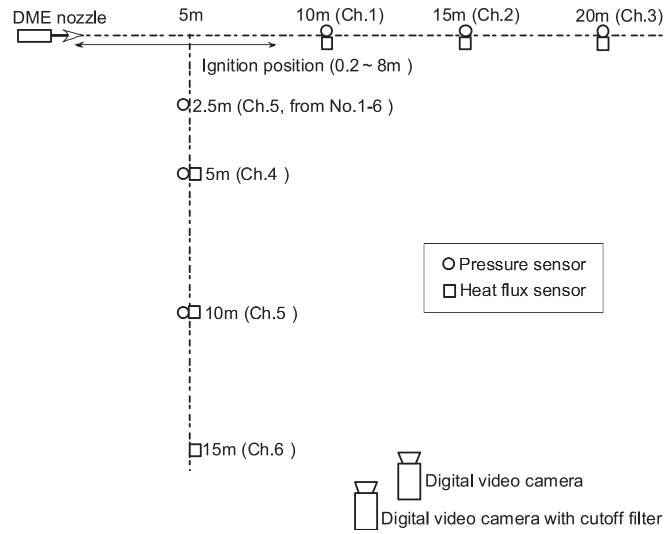

Fig. 2. Arrangement of sensors.

3. Results and discussion

3.1. Ignition and flame propagation

The experiments were carried out in summer (average temperature: 303 K, humidity: 46%, wingless). The initial reservoir pressure without pressurization by nitrogen gas was higher than the vapor pressure of DME (0.68 MPa at 303 K), because the pipe was heated by solar heat. In the present experiments, the total amount of released liquid DME was approximately 1 kg for all cases.

Table 1 lists the experimental conditions and results. The parameters consisted of the following four items:

- ignition method (pilot burner or electric spark)
- ignition position (distance from the leakage nozzle to ignition source; $x_{ig} = 0.2–8$ m)
- initial reservoir pressure (vapor pressure or 2 MPa)
- time to turn on the ignition source ($t_{ig} = 0–1.75$ s).

The results include whether ignition occurred, the duration time of the DME release, and elapsed time from the start of leakage to ignition. The duration of the DME release was obtained from the time history of the release pressure. The duration of the DME release was approximately constant for all cases. Furthermore, ignition was achieved before the DME release was stopped in almost cases. In the case of Test No. 3-3, the DME jet did not ignite. It seems that the DME was a liquid near the nozzle, and the electrode was located on the jet axis.

Typical video images of dispersion and flame propagation of liquid DME are shown in Fig. 3. Time zero denotes the time at which the air operating valve is opened. The ignition position was varied but the ignition source was the pilot burner when the ignition position was $x_{ig} = 0.2$ m (Test No. 3-4). The flame was spherical near the ignition position, but expanded along the discharge axis. The flame is yellow and has high luminance, whereas the flame of DME generally has low luminance, because little soot is generated by combustion. However, if the ignition position was far from the nozzle, the luminance of the flame was weak. The DME concentration is considered to have become low until the point of ignition because of dilution by mixing with air and the diffusion of DME.

The variation of the flame tip with time is shown in Fig. 4 when the spouting pressure was 2 MPa but the ignition position differed for each experiment. The results were image-based measurements

Table 1
Experimental conditions and results.

Test no.	Reservoir pressure P [MPa]	Ignition source	Time elapsed from start of leakage to turning on ignition source t_{ig} [s]	Ignition position x_{ig} [m]	Ignition/non ignition	Duration time of DME release t [s]	Time elapsed from start of leakage to ignition τ_{ig} [s]
1-1	1.25	Pilot burner	0 (Beforehand)	0.2	Ignition	0.93	0.10
1-2	1.0	Pilot burner	0	1	Non ignition	0.89	–
1-3	1.0	Pilot burner	0	4	Ignition	0.90	0.27
1-4	1.0	Pilot burner	0	5	Ignition	0.85	0.63
1-5	1.1	Pilot burner	0	6	Ignition	0.83	0.67
1-6	1.1	Pilot burner	0	7	Ignition	0.91	0.60
1-7	1.1	Pilot burner	0	8	Non ignition	0.86	–
2-1	1.1	Electric spark	0	2	Ignition	0.88	0.20
2-2	1.0	Electric spark	0	3	Ignition	0.91	0.17
2-3	1.0	Electric spark	0	4	Ignition	0.79	0.33
2-4	1.0	Electric spark	0	5	Ignition	0.93	0.40
2-5	1.0	Electric spark	0	6	Ignition	0.97	0.53
2-6	1.0	Electric spark	0	7	Non ignition	0.85	–
3-1	2.0	Electric spark	0	3	Ignition	0.83	0.40
3-2	2.0	Electric spark	0	6	Ignition	0.85	0.47
3-3	2.0	Electric spark	0	0.2	Non ignition	0.83	–
3-4	2.0	Pilot burner	0	0.2	Ignition	0.68	0.03
4-1	1.0	Electric spark	0.75	5	Ignition	0.84	0.77
4-2	0.97	Electric spark	1.75	5	Non ignition	0.78	–
4-3	0.97	Electric spark	0.75	6	Ignition	0.85	0.87

of the distance from the nozzle to the flame tip on the horizontal axis. This distance is also shown for the DME jet, but the white smoke generated by vaporized DME is regarded as the tip of the jet. The images were obtained from 16 to 51 visible and successive frames with an interval of 1/30 s. The variation of the flame tip is considered to be similar to the tip of the DME jet.

Velocity profiles of the DME jet and flame propagation are shown in Fig. 5. The conditions were the same as in Fig. 4. Each data point corresponds to the average velocity between each frame. In all cases, the velocity near the ignition position is the fastest. In the case of Test No. 3-2, $x_{ig} = 3$ m, the maximum flame propagation velocity is faster than in other cases. It appears that

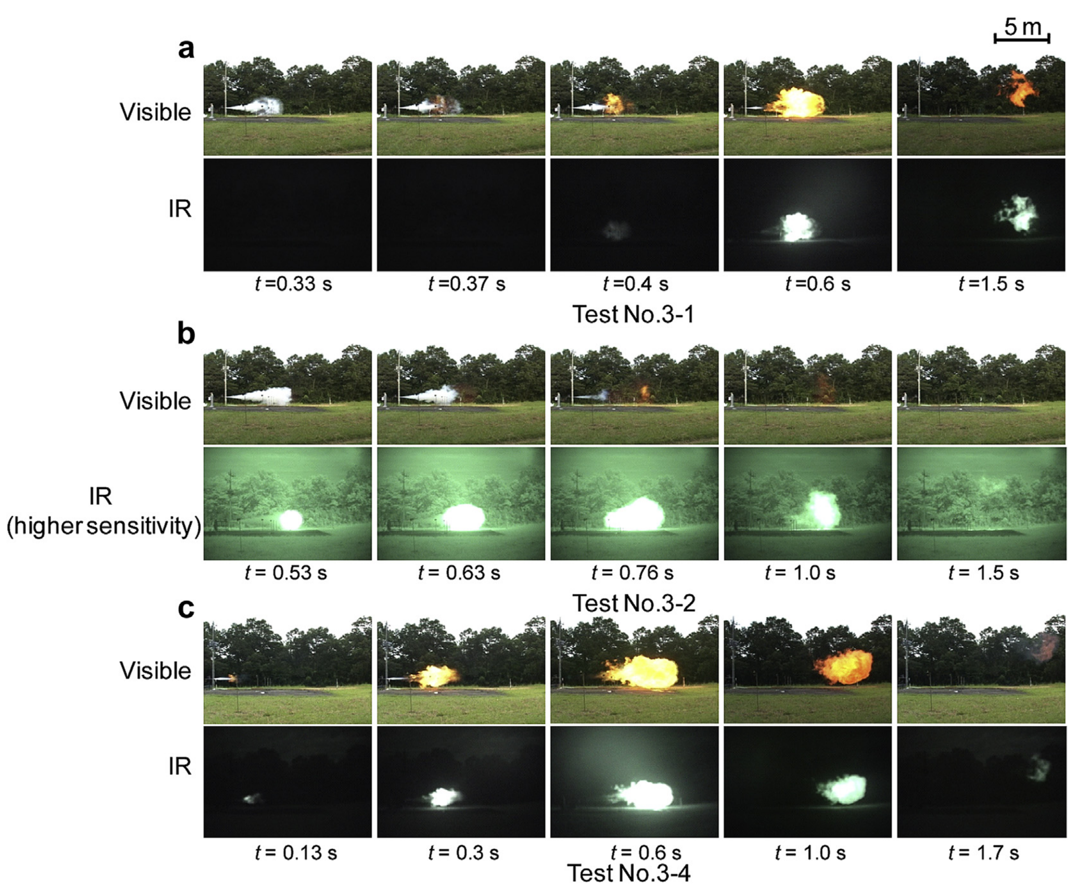

Fig. 3. Video images of flame propagation of discharging liquid DME.

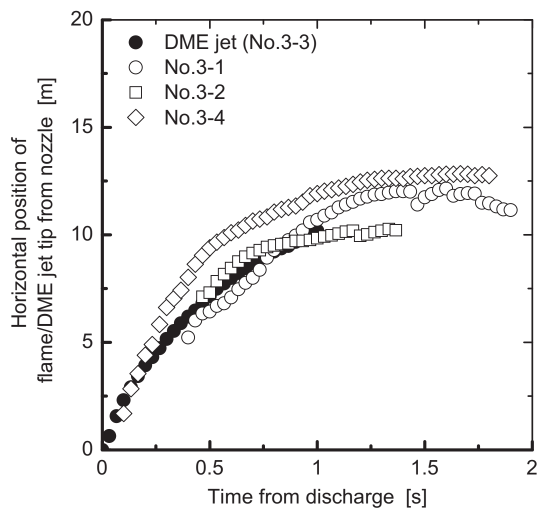

Fig. 4. Variation of flame tip and DME jet with time.

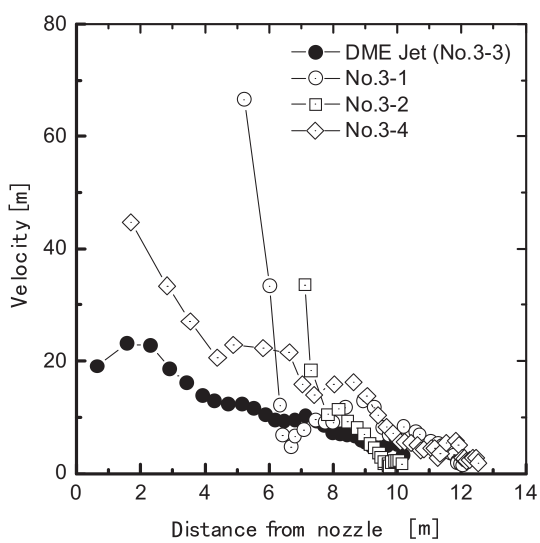

Fig. 5. Velocity profiles of flame propagation and DME jet.

the DME and the surrounding air are mixed and nearly stoichiometric mixture is formed because the ignition position is moderately separated from the nozzle. In contrast, near the nozzle, the initial turbulence is significant. However, liquid DME is vaporized, and the concentration is very high. Therefore, it appears that the flame propagation velocity does not become as high as the DME jet velocity.

Fig. 6(a) shows the relation between the maximum arrival distance of the flame tip of the propagating flame and the ignition position. The relation between duration of combustion and the ignition position is also shown in Fig. 6(b). When ignition occurs near the nozzle, the flame tip tends to extend farther from the nozzle. Furthermore, the duration of combustion tends to increase. Hasegawa and Sato (1978) have obtained the following experimental equation on the duration of the fireball resulting from unconfined vapor cloud explosions of hydrocarbon (fuel mass: 3.1–31.0 kg, propane, pentane, and octane):

$$\tau = 1.07M^{0.181} \tag{1}$$

where τ (s) is the fireball duration and M (kg) is the mass of the release. Furthermore, Fay and Lewis (1977) have reported the following equation obtained by unconfined vapor cloud explosions of gaseous propane (fuel mass 0.04–0.36 g):

$$\tau = 2.51M^{1/6} \tag{2}$$

These studies have reported that the fireball duration is dependent on the fuel mass of the release. Furthermore, their ignition positions are fixed regardless of the experimental conditions. However, in this experiment, the fireball duration decreased as the distance between the nozzle and the ignition position increased. In other words, the fireball duration changes with the ignition position although the fuel mass remains the same. The reason for this is considered to be as follows. When ignition occurs at a position at which the DME concentration is low, the flame cannot propagate to upstream because the burning velocity is smaller than the jet velocity. As a result, the fireball duration decreases if the ignition position becomes far from the nozzle.

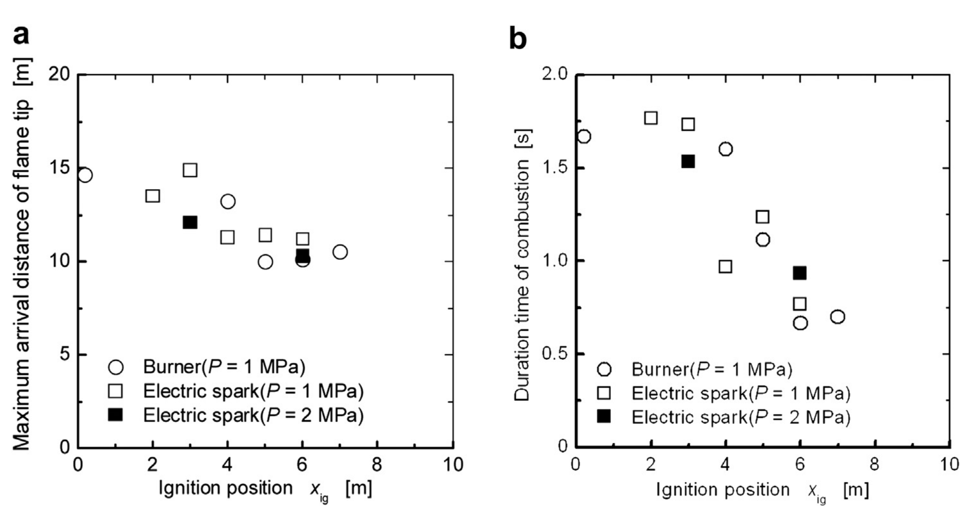

Maximum arrival distance of flame tip Duration time of combustion

Fig. 6. Properties of flame propagation.

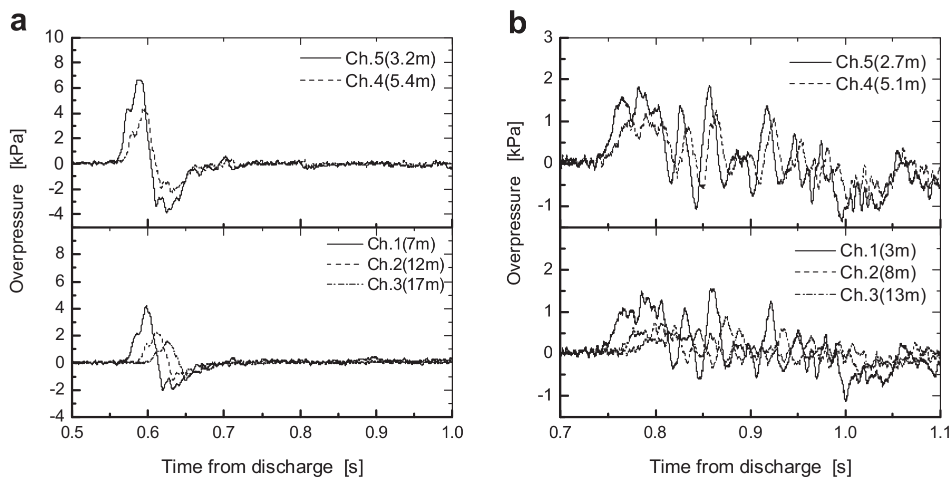

Test No.3-1 Test No.3-2

Fig. 7. Typical pressure wave histories at each sensor.

3.2. Blast wave generated by the propagating flame

Typical pressure wave histories at each sensor are shown in Fig. 7. In the case of Test No. 3-1, the blast pressure wave rapidly increases with time, and the overpressure at a distance of 3.2 m from the ignition position is high, i.e., exceeding 6 kPa. Just after peaking, the blast wave pressure immediately decreases to become negative. On the other hand, when ignition occurs far from the nozzle, as in the case of Test No. 3-2, following the initial pressure peak (>1.5 kPa), pressure waves of almost the same strength are sustained repeatedly.

Fig. 8 shows the relation between the peak overpressure and the distance from the ignition positions when the ignition method and the reservoir pressure were varied. Fig. 8(a) shows the results for the axis, and Fig. 8(b) shows the results for the comparison between the axis and the side in the cases of Test No. 3-1 and Test No. 3-2. The peak overpressure is observed to be independent of the ignition position and the direction of the measurement position. In other words, the blast strength is not influenced by the DME concentration at the ignition position or the direction from the DME jet.

In order to estimate the value of the blast wave induced by the explosion of the discharged DME, it was compared with the values of the blast wave obtained by deflagration and detonation using a DME/air mixture (LPG Research Laboratory of the High Pressure Gas Institute (KHK), 2005). A deflagration test was performed using a rectangular-shaped plastic tent (81 m^3) filled with stoichiometric mixtures of DME and air (6.5% DME by volume in theory), and the mixture was ignited by an electric spark at center of the tent. A detonation test was performed using a cylindrical plastic tent having a volume of 7.74 m^3. The mixture was stoichiometric and was ignited by a detonating explosive (0.18 kg of pentolite) located at center of the tent.

The scaled peak overpressure ($(P_{max} - P_0)/P_0$) is shown as a function of the scaled distance (R/R_0) for each experiment in Fig. 9. Here, the characteristic distance is defined as $R_0 = (E/P_0)^{1/3}$, where P_0 is the ambient pressure, and E is the lower heating value of the volume of the DME/air mixture. The results indicate that the blast wave from the fireball of leaked DME is higher than that from deflagration by DME/air mixture. When the release pressure is 1 MPa, the overpressure from the fireball is a hundred times smaller than that from the detonation. The blast wave from the fireball is

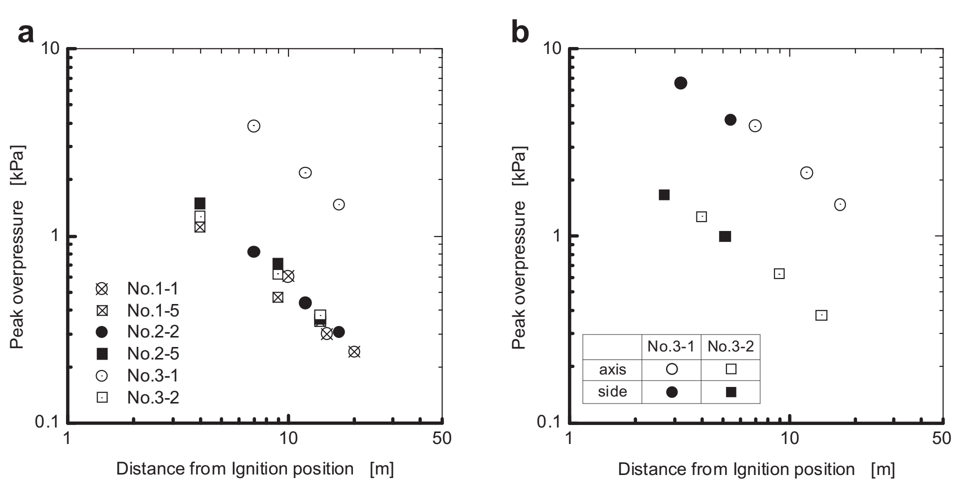

Peak overpressure on the axis of the Jet Comparison between the axis and the side.

Fig. 8. Relation between peak overpressure and distance from the ignition positions.

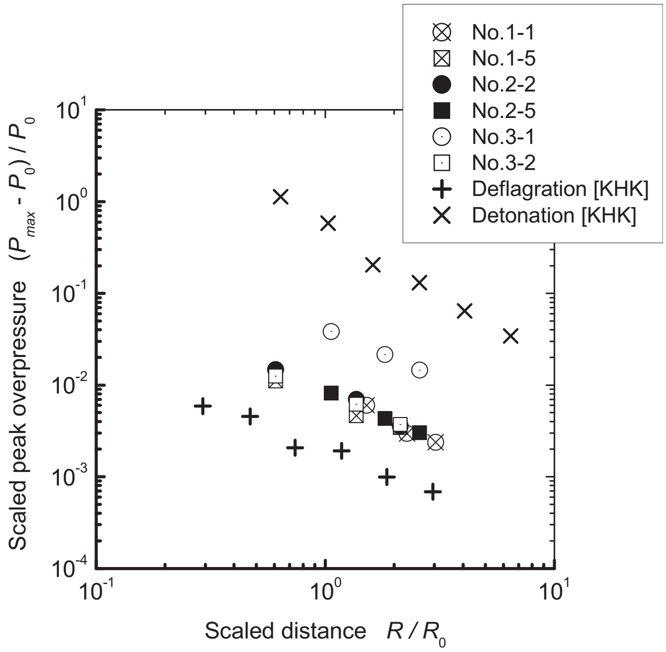

Fig. 9. Comparison between scaled peak overpressure from the fireball of discharged DME and scaled peak overpressure by deflagration or detonation of DME/air mixture.

considered to be higher than that from deflagration because the flow of DME discharged from the nozzle was turbulent and the flame propagation velocity increased.

3.3. Thermal radiation hazards

Fig. 10 shows the relation between the maximum heat flux and the distance from the discharge axis. The maximum heat flux is measured by each sensor at the side of the flame. Although the discharged fuel mass in all cases was same, the maximum heat flux differed for each experimental condition. In other words, when DME ignites far from the nozzle, the heat flux from the fireball becomes small. Hasegawa and Sato (1978) reported the experimental equation correlated with the maximum radiation flux, E_{max} (W/m^2), the distance between the fireball and the detector, L (m), and the hydrocarbon fuel mass, M (kg), as follow:

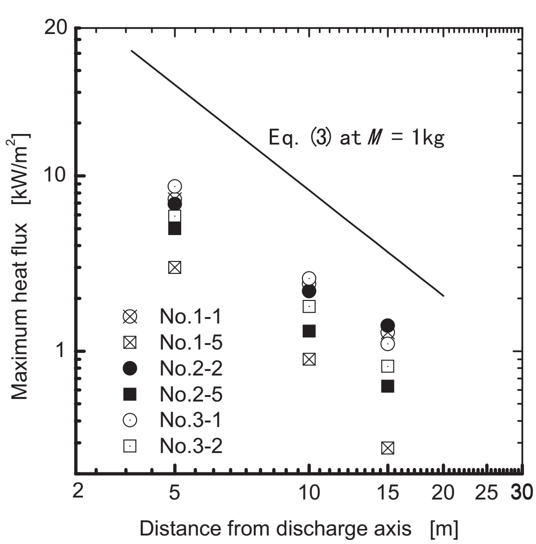

Fig. 10. Relation between maximum heat flux and the distance from discharge axis.

$$(E_{max})L^2 = 8.28 \times 10^5 M^{0.771} \tag{3}$$

Although Eq. (3) indicates that the radiation heat flux is constant if the distance between the fireball and the detector and remain unchanged, the radiation heat flux from the fireball changes with the ignition position, although the fuel mass is the same. The DME is considered to be diluted until the ignition and the combustion efficiency becomes small. On the other hand, the line in Fig. 10 shows the data obtained by Eq. (3) when the fuel mass is 1 kg. Since the generation of soot in DME combustion is small, the heat flux from the fireball generated by DME combustion is smaller than that generated by the hydrocarbon fuel.

4. Conclusions

Field experiments were carried out to examine the leakage and explosion of liquid DME, in which we assumed that a filling hose or pipe at a DME filling station was broken. The ignition method, ignition position, and reservoir pressure of DME were varied. Flame propagation, blast pressure, and radiant heat flux data could be obtained. The results indicate that the duration time and the radiant heat flux from the fireball are dependent on the ignition position. The overpressure resulting from the vapor cloud explosion of DME is larger than that from the gas explosion caused by spherical flame propagation. These results can be used for risk assessment in facilities that handle liquid DME and can be used in the consideration of safety measures.

Acknowledgment

The authors would like to thank the Kanto Bureau of Economy, Trade and Industries for supporting the present study as part of a program on the research and development of DME filling devices for cars and safety research on DME filling stations.

References

Bubbico, R., & Marchini, M. (2008). Assessment of an explosive LPG release accident: a case study. *Journal of Hazardous Materials, 155*, 558–565.
Daly, C. A., Simmie, J. M., & Wurmel, J. (2001). Burning velocities of dimethyl ether and air. *Combustion and Flame, 125*, 1329–1340.
Fay, J. A., & Lewis, D. H. (1977). Unsteady burning of unconfined fuel vapor clouds. *Proceedings of the Combustion Institute, 16*, 1397–1403.
Hasegawa, K., & Sato, K. (1978). *Experimental investigation of the unconfined vapour-cloud explosions of hydrocarbons, Vol. 12*. Tokyo: Tech Memos Fire Research Institute of Japan, (pp. 3–9).
Huang, Z., Wang, Q., Yu, J., Zhang, Y., Zeng, K., Miao, H., et al. (2007). Measurement of laminar burning velocity of dimethyl ether–air premixed mixtures. *Fuel, 86*, 2360–2366.
LPG Research Laboratory of the High Pressure Gas Institute (KHK). (2005). *The report of basic research on practical application of DME fuel* (in Japanese).
Mogi, T., & Horiguchi, S. (2009). Explosion and detonation characteristics of dimethyl ether. *Journal of Hazardous Materials, 164*, 114–119.
Nifuku, M., Barre, C., Fujiwara, S., Horiguchi, S., Hatori, M., Nanba, M., et al. (2006). An investigation on the static electrification of dimethyl ether. *Journal of Electrostatics, 64*, 471–476.
Suha, H. K., & Lee, C. S. (2008). Experimental and analytical study on the spray characteristics of dimethyl ether (DME) and diesel fuels within a common-rail injection system in a diesel engine. *Fuel, 87*, 925–932.
Yamada, H., Yoshii, M., & Tezaki, A. (2005). Chemical mechanistic analysis of additive effects in homogeneous charge compression ignition of dimethyl ether. *Proceedings of the Combustion Institute, 30*, 2773–2780.
Ying, W., Li, H., Jie, Z., & Longbao, Z. (2009). Study of HCCI-DI combustion and emissions in a DME engine. *Fuel, 88*, 2255–2261.
Zhao, Z., Kazakov, A., & Dryer, F. L. (2004). Measurements of dimethyl ether/air mixture burning velocities by using particle image velocimetry. *Combustion and Flame, 139*, 52–60.